

Intrinsic Functional Relations Between Human Cerebral Cortex and Thalamus

Dongyang Zhang,¹ Abraham Z. Snyder,^{1,2} Michael D. Fox,¹ Mark W. Sansbury,¹ Joshua S. Shimony,¹ and Marcus E. Raichle^{1,2,3,4,5}

¹Department of Radiology, ²Department of Neurology, ³Department of Neurobiology, ⁴Department of Psychology, and ⁵Department of Biomedical Engineering, Washington University, St. Louis, Missouri

Submitted 14 April 2008; accepted in final form 10 August 2008

Zhang D, Snyder AZ, Fox MD, Sansbury MW, Shimony JS, Raichle ME. Intrinsic functional relations between human cerebral cortex and thalamus. *J Neurophysiol* 100: 1740–1748, 2008. First published August 13, 2008; doi:10.1152/jn.90463.2008. The brain is active even in the absence of explicit stimuli or overt responses. This activity is highly correlated within specific networks of the cerebral cortex when assessed with resting-state functional magnetic resonance imaging (fMRI) blood oxygen level–dependent (BOLD) imaging. The role of the thalamus in this intrinsic activity is unknown despite its critical role in the function of the cerebral cortex. Here we mapped correlations in resting-state activity between the human thalamus and the cerebral cortex in adult humans using fMRI BOLD imaging. Based on this functional measure of intrinsic brain activity we partitioned the thalamus into nuclear groups that correspond well with postmortem human histology and connectional anatomy inferred from nonhuman primates. This structure/function correspondence in resting-state activity was strongest between each cerebral hemisphere and its ipsilateral thalamus. However, each hemisphere was also strongly correlated with the contralateral thalamus, a pattern that is not attributable to known thalamocortical monosynaptic connections. These results extend our understanding of the intrinsic network organization of the human brain to the thalamus and highlight the potential of resting-state fMRI BOLD imaging to elucidate thalamocortical relationships.

INTRODUCTION

Spontaneous fluctuations of the blood oxygen level–dependent (BOLD) functional magnetic resonance imaging (fMRI) signal are temporally coherent within anatomically and functionally related areas of the brain (e.g., see Damoiseaux et al. 2006; Fox et al. 2005; Greicius et al. 2003; Hampson et al. 2002; Vincent et al. 2007). Functionally organized systems defined on this basis were first described by Biswal and colleagues (1995) within the somatomotor network and since then have been demonstrated in multiple systems within the cerebral cortex (for a recent comprehensive review of this literature see Fox and Raichle 2007). Less is known regarding participation of the thalamus in this intrinsic activity despite its central role in the function of the cerebral cortex (Jones 2007; Sherman and Guillery 2006).

Given the unique cytoarchitecture and firing patterns in the thalamus (Jones 2007; Sherman and Guillery 2006), it is unclear whether and how spontaneous BOLD fluctuations in the thalamus and cortex will be related. Previous resting-state functional connectivity studies using fMRI BOLD imaging

have occasionally noted significant thalamocortical correlations (Anand et al. 2005; Beckmann et al. 2005; De Luca et al. 2006; Dosenbach et al. 2007; Fox and Raichle 2007; Greicius et al. 2007; Seeley et al. 2007; Stein et al. 2000). However, in many cases, the observed correlations extended over large areas of the thalamus without respecting classical nuclear boundaries and there has been no attempt to systematically characterize thalamic nuclei on the basis of spontaneous activity. The lack of specificity with regard to the thalamus in prior resting-state BOLD correlation mapping likely reflects not only shared neuronal signals propagated over multiple brain areas but also spatially uniform fluctuations in the BOLD signal generated by cardiac and respiratory activity (Birn et al. 2006; Triantafyllou et al. 2005).

The present work examines patterns of coherence within the thalamocortical system derived from partial correlation mapping of spontaneous fluctuations in the fMRI BOLD signal. Highly specific patterns of resting-state connectivity were seen between specific regions of the cerebral cortex and the thalamus. Much of the observed functional connectivity reflects known anatomical connections, consistent with evidence that resting-state networks are synchronized by the underlying axonal connections (Greicius et al. 2008; Honey et al. 2007; Johnston et al. 2008; Quigley et al. 2003; Vincent et al. 2007). However, some aspects of the connectivity (e.g., the bilaterally symmetric correlations of the cerebral cortex in the thalamus) are uniquely revealed by this imaging approach, adding a new dimension to our understanding of the organization of the brain's intrinsic activity.

METHODS

Resting-state BOLD sensitized fMRI data ($4 \times 4 \times 4$ mm voxels, TE 25 ms, TR 2.16 s) were acquired in 17 normal young adults using a 3T Siemens Allegra MR scanner in the course of a previous study (Fox et al. 2007). Each data set included four 7-min runs of 194 frames each (28 min total) during which subjects visually fixated on a crosshair. No task was imposed except to remain still and not fall asleep.

Structural images acquired for definitive atlas transformation included a $1 \times 1 \times 1.25$ -mm sagittal T1-weighted magnetization-prepared rapid gradient echo (MP-RAGE) (TR = 2.1 s, TE = 3.93 ms, flip angle = 7°) and a T2-weighted (T2W) fast spin echo scan.

Preprocessing of imaging data

Preprocessing included compensation for systematic, slice dependent time shifts using sinc interpolation, elimination of systematic

Address for reprint requests and other correspondence: D. Zhang, Washington University, Department of Radiology, Campus Box 8225, 510 South Kingshighway Blvd., St. Louis, MO 63110 (E-mail: zhangd@npg.wustl.edu).

The costs of publication of this article were defrayed in part by the payment of page charges. The article must therefore be hereby marked "advertisement" in accordance with 18 U.S.C. Section 1734 solely to indicate this fact.

odd-even slice intensity differences due to interleaved acquisition, rigid body correction for head motion within and across runs, and normalization of the signal intensity across each run (not counting the first four frames) to obtain a whole brain mode value of 1,000 (Ojemann et al. 1997). Atlas transformation was achieved by composition of affine transforms connecting the first functional volume (averaged over all fMRI runs after cross-run realignment) with the T2-weighted and T1-weighted structural images. Common mode image registration (e.g., to correct for head motion within and across fMRI runs and affine warping of T1-weighted structural images to the atlas-representative target image) was performed using in-house versions of standard algorithms (Woods et al. 1998). Cross-modal registration (e.g., T2- to T1-weighted images) was performed using the vector gradient matching algorithm of Rowland et al. (2005). Our atlas-representative template includes MP-RAGE data from 12 normal individuals and was made to conform to the 1988 Talairach atlas (Talairach and Tournoux 1988) according to the method of Lancaster et al. (1995). To prepare our BOLD data for the present analyses, each fMRI run was resampled to 2-mm³ voxels in atlas space. For display purposes, voxel boundaries were smoothed using fourfold interpolation and then displayed using in-house software written on the MATLAB platform (The MathWorks, Natick, MA).

Linear trends across runs were removed voxelwise and the data were low-pass filtered using a second-order Butterworth filter to retain frequencies <0.1 Hz. No high-pass filter was used. Several sources of spurious variance were removed by regression of the following nuisance variables along with their first derivatives: 1) the six parameters resulting from rigid body correction for head motion; 2) a signal from a ventricular region of interest (ROI); 3) and a signal from a white-matter ROI (Fox et al. 2005). Regression of the whole brain signal, which normally is included in our seed ROI-based functional connectivity procedure (Fox et al. 2005), was omitted because of our observation that the thalamus highly correlates with this signal (D Zhang and MD Fox, unpublished observations). Spatial blurring was also omitted to maximize resolution in the analyses of small brain structures, in particular the thalamus.

Cortical ROI definition

To investigate the specific functional relationships between the cortex and the thalamus, the cortex of each hemisphere was partitioned into five disjoint regions. In detail, the MP-RAGE image obtained in a normal young adult volunteer (not included in this study) was segmented and the brain surface extracted and deformed to the population-average, landmark- and surface-based (PALS)-B12 (Van Essen 2005) atlas using SureFit and CARET (Van Essen and Drury 1997; Van Essen et al. 2001). The partition boundaries were manually drawn on the basis of major sulcal landmarks, largely following previous work (Behrens et al. 2003) taking into account the known anatomical connectivity of the thalamus and the cortex. In this manner, five disjoint cortical ROIs were defined: 1) frontopolar and frontal cortex including the orbital surface and anterior cingulate; 2) motor and premotor cortex (Brodmann areas 6 and 4) excluding adjacent portions of cingulate cortex; 3) somatosensory cortex (Brodmann areas 3, 1, 2, 5, and parts of 40); 4) parietal and occipital cortex including posterior cingulate and lingual gyrus; 5) temporal cortex including the lateral surface, temporal pole, and parahippocampal areas (Fig. 1A). All of the insula and adjacent opercular regions as well as midcingulate cortex were excluded from the present analyses. To generate five volume space ROIs, the surface regions obtained by the partitioning scheme were assigned a thickness of 3 mm (1.5 mm above and below the fiducial surface corresponding to "layer IV").

Partial correlation mapping between the cerebral cortex and the thalamus

The average BOLD time course was extracted from each cortical ROI. Using these time courses, partial and total correlations were

computed for each voxel in the thalamus. The equations for total and partial correlations appear in supplemental material.¹ We computed partial correlations between each thalamic voxel and each of five cortical ROIs. The partial correlation between the local thalamic signal and cortical ROI 1 is the correlation after *eliminating the influence of all other cortical ROIs*. It should be noted that partial correlation can be related to regression and total correlation by the following example. For given signals A, B, and C, the partial correlation of A and B eliminating the influence of C is the same as regressing the influence of C from A and B, and then computing the total correlation of the residuals of A and B.

For purposes of calculating statistical significance, partial correlation coefficients were converted to a normal distribution using Fisher's *r*-to-*z* transform. In computing the statistical significance of correlations when successive observations are independent, the degree of freedom is equal to the number of samples less a small correction. However, since consecutive BOLD frames are not independent, it is necessary to correct the degrees of freedom according to Bartlett's theory (Fox et al. 2005; Jenkins and Watts 1968). In the present data, the proportionality between frames and degrees of freedom was computed to be 3.183. Accordingly, for purposes of significance testing under a fixed-effects model, the *z*-transformed partial correlation values were converted to *Z*-scores by multiplying by $\sqrt{(n - k - 3)}$, where *n* is the degrees of freedom (number of frames divided by 3.183) and *k* is the order of the partial correlation (places to the right of the point in Yule's notation in Eq. 3; see supplemental material) (Weatherburn 1949). It should be noted that statistical parametric mapping is an alternative, equally valid method to partial correlation mapping (Friston 2007). *Z*-score maps were combined across subjects using a fixed-effects analysis. Although partial correlations are defined over all voxels in the brain, we confine the reporting of our results to the thalamus, superior and inferior colliculi, striatum, and globus pallidus. Boundaries enclosing these structures were created by manual tracing of the atlas template. Resulting images were corrected for multiple comparisons using a bootstrap method (see supplemental materials).

RESULTS

Thalamus mapping

Results obtained by partial correlation mapping of the thalamus are shown in Fig. 1 and Supplemental Fig. S2. Each cortical ROI representing bilaterally homologous areas of the cerebral cortex gave rise to significantly positive partial correlations in spatially restricted zones of the thalamus. Moreover, inspection of all five partial correlation maps revealed that most voxels within the thalamus showed strongly positive, nonoverlapping correlations with one and only one cortical ROI. Thus for example, the map of the somatosensory ROI (Fig. 1B, panel 4) showed strong positive correlations in a zone corresponding to a void in the motor + premotor map (Fig. 1B, panel 3). Systematic evaluation of the partial correlation of each thalamic voxel with each of the five cortical ROIs (Fig. 2) confirmed that the great majority of thalamic voxels were strongly positively correlated with one and only one cortical ROI. This nonoverlapping property suggested creating winner-take-all (WTA) representations by labeling each thalamic voxel according to the cortical ROI with the highest partial correlation (Fig. 1C and Supplemental Fig. S3). The WTA maps were highly ordered: similarly labeled voxels were clustered together in aggregate regions, suggesting thalamic nuclear groups.

¹ The online version of this article contains supplemental data.

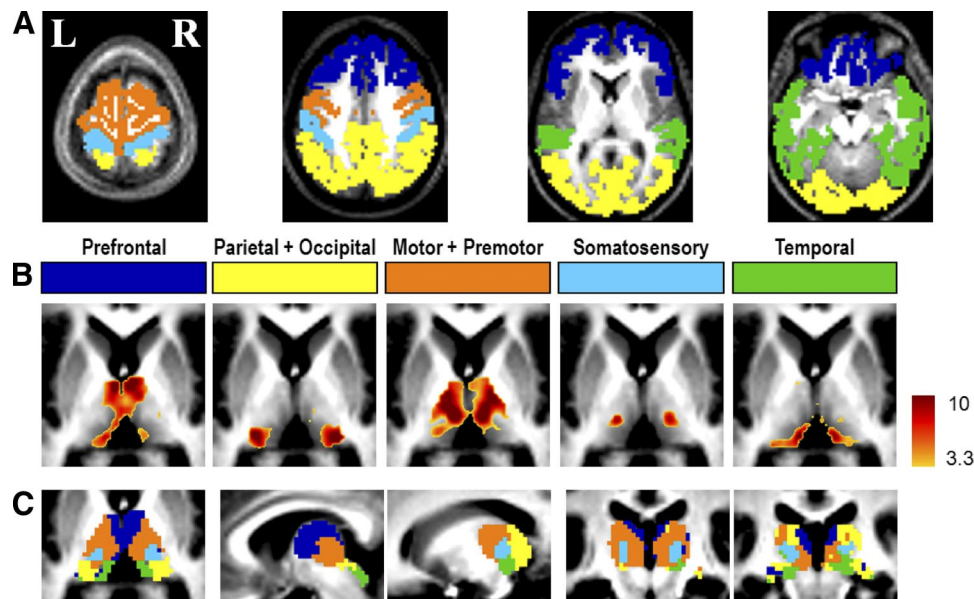


FIG. 1. Highly specific correlations are seen between the cerebral cortex and the thalamus in their intrinsic activity. *A*: bilateral cortical regions of interest (ROIs) illustrating partitioning according to major anatomical landmarks. Prefrontal: dark blue; Parietal + Occipital: yellow; Motor + Premotor: orange; Somatosensory: light blue; Temporal: green. This color code is consistently used in all figures. Selected transverse slices ($z = 66, 39, 9, -18$) are shown. *B*: partial correlation Z-score maps (fixed-effects analysis using all 17 subjects) generated for each of the cortical ROIs. Voxels meeting a criterion of $P < 0.05$ are colored. Transverse slice $z = 6$. Note: spatially distinct maps for each of the cortical ROIs. See supplemental data for localization of negative partial correlations and a discussion on the interpretation of negative partial correlations. *C*: winner-take-all (WTA) maps obtained by labeling each thalamic voxel according to the cortical ROI with the highest partial correlation value. Only voxels at which the most winning Z-score significance exceeded $P < 0.05$ are colored (color code as in *A*). From left to right: transverse slice $z = 6$; sagittal slices $x = 5, 15$; coronal slices $y = -23, -27$.

Closer inspection of our partial correlation results suggested a substantial correspondence with known axonal connectivity determined by postmortem human studies (Morel et al. 1997) and extrapolated from monkey studies (Jones 2007; Nieuwenhuys et al. 1988). Summarized briefly, previously established anatomical results document reciprocal connections between the prefrontal cortex and mediodorsal nucleus; the motor and premotor cortex with ventral anterior and ventral lateral nuclei; the somatosensory cortex with ventral posterior nucleus; the temporal cortex with medial pulvinar and medial geniculate nucleus (MGN); occipital cortex with the lateral geniculate nucleus (LGN); and occipital and parietal cortex with the inferior pulvinar (Jones 2007). The superior colliculus is a subcortical eye-movement control center that is reciprocally connected with the visual (occipital) cortex (Lock et al. 2003), whereas the inferior colliculus is an auditory relay center reciprocally connected with auditory (temporal) cortex (Herbert et al. 1991; Roger and Arnault 1989). The present partial correlation results (Fig. 1, *B* and *C* and Supplemental Figs. S2 and S3) bear comparison to the above-summarized connective neuroanatomy with the caveat that the spatial resolution of fMRI is coarse compared with histology. Thus in the following discussion of thalamic nuclear groups the precision is necessarily approximate. Proceeding on this basis, the parietal + occipital cortical ROI (yellow label) showed maximal partial correlation with a subdivision of the thalamus that provisionally corresponds to the lateral pulvinar as well as the superior colliculus (Fig. 1*C*). The temporal cortical ROI corresponded most strongly with what appears to be the medial pulvinar as well as the inferior colliculus. Similarly, the prefrontal cortical ROI (dark blue label) showed maximal partial correlation with mediodorsal and anterior nuclear areas. The locus of maximal correlation of the somatosensory cortical

ROI (light blue) seems to correspond approximately to nucleus ventral posterior (VP; see Supplemental Fig. S3, coronal view). The motor cortical ROI correlated with a large region of the thalamus that includes what seems to be the ventral lateral, ventral anterior, and parts of mediodorsal nuclei.

Anatomically, the motor areas of cortex that connect with basal ganglia regions such as the putamen also connect with intralaminar nuclei, which in turn project fibers to the same areas of putamen (Jones 2007). Extending our maps to include the basal ganglia showed that motor/premotor cortex was correlated with both the putamen and parts of intralaminar nuclei that included the centre median nucleus (Fig. 3). The caudate nucleus correlated most strongly with the prefrontal ROI. Globus pallidus, which receives anatomical projections from striatum, did not correlate with associated cortical ROIs either in the prefrontal or motor/premotor areas, although neurotransmission to globus pallidus is inhibitory (GABAergic), whereas all other pathways mentioned thus far are excitatory (glutamatergic). Only the parietal + occipital ROI showed correlations with parts of globus pallidus, specifically the internal segment (Fig. 3). Direct seeding of the internal segment approaches the limit of our spatial resolution but direct seeding of the putamen, which is a much larger structure, clearly showed that the putamen is not correlated with the GP, although it was correlated with contralateral putamen and also with ventral anterior/ventral lateral thalamic nuclei (Supplemental Fig. S4).

Because most thalamic voxels exhibit strong partial correlations with one and only one cortical ROI (Fig. 2), the WTA representation is efficient and mostly accurate. However, some thalamic nuclei showed strong partial correlation with two cortical ROIs. In particular, the medial pulvinar's spontaneous activity contained signals unique to both the prefrontal and

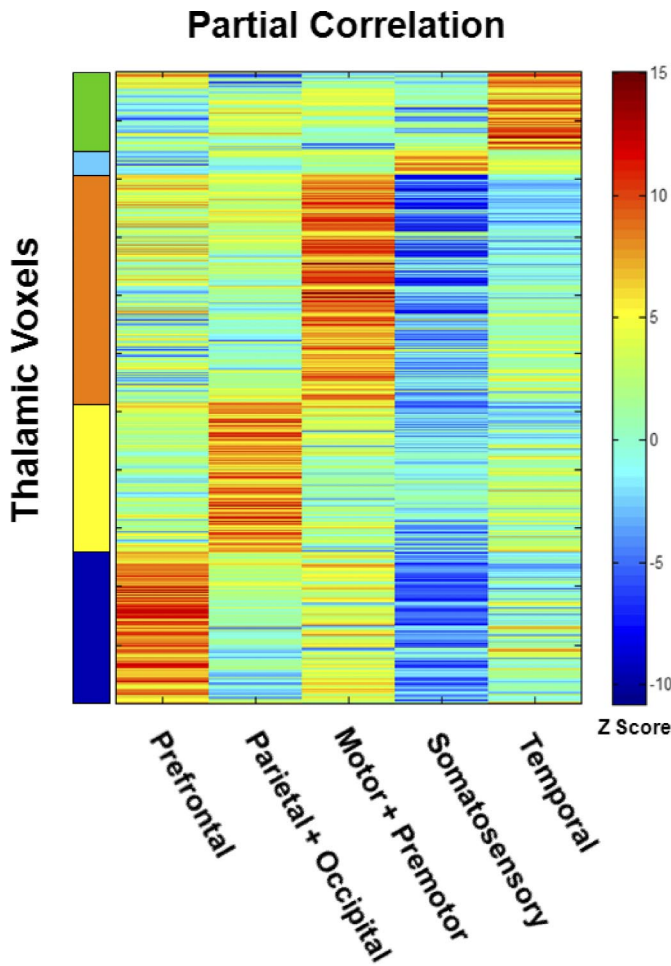


FIG. 2. Each thalamic voxel is highly correlated with one cortical ROI. This matrix represents partial correlations computed for each thalamic voxel paired with each cortical ROI. First, correlation values were computed for each subject and transformed using Fisher's *r*-to-*z* transform. Then, descriptive Z-scores were generated at the population level using a fixed-effects model (see METHODS). Red and blue hues indicate, respectively, positive and negative correlations. Thalamic voxels within the same WTA bilateral thalamic partition (Fig. 1C) are grouped together on the vertical axis.

temporal ROIs (Fig. 1B, panels 1 and 5), suggesting that this thalamic locus intrinsically communicates with both cortical areas. Connectional anatomy supports this observation with evidence that the medial pulvinar is strongly interconnected with both temporal and prefrontal cortex (Nieuwenhuys et al. 1988).

Laterality of partial correlations

Because the above-discussed results were obtained with bilaterally symmetric cortical regions that were necessarily

highly symmetric, we next repeated the partial correlation analysis using cortical ROIs confined to one hemisphere. The results obtained with unilateral cortical ROIs (Fig. 4 and Supplemental Fig. S5) were surprisingly similar to the maps obtained with bilateral ROIs in their spatial distribution (Fig. 1). In particular, only modest asymmetry was present. To quantitatively assess asymmetry in partial correlation strength, thalamic voxels were first partitioned on the basis of the WTA map shown in Fig. 1C. Then, the partial correlations were computed for each WTA partition and its corresponding cortical ROI and then transformed using Fisher's *r*-to-*z* transform. A random-effects analysis was conducted against the null hypothesis of no statistical difference between partial correlations involving unilateral cortical ROIs and either hemithalamus.

This statistical maneuver returned highly significant results for the prefrontal partial correlations (Table 1; dark blue label). Quantitatively moderate and borderline significant ipsilaterality was also seen in the motor + premotor (orange) and in the somatosensory (light blue) results. Interestingly, parietal + occipital correlations (yellow) were always stronger in the right thalamus, regardless of whether the cortical ROI was in the left or right hemisphere. Thalamic partial correlations with the temporal ROI (green) were notable for the complete absence of laterality.

Total and partial correlations

In our analysis, we sought to eliminate the shared influence from a priori regions of interest, specifically the influence from other cortical ROIs. A comparison was made to correlation maps generated without eliminating these shared influences (total correlation maps) to see how partial correlation differed from a more traditional approach (see Fox et al. 2005; Vincent et al. 2006). Starting from the same cortical regions, partial correlation maps showed increased specificity relative to total correlation maps, especially in the motor/premotor and somatosensory maps (Fig. 5). These two cortical regions have very similar BOLD profiles and therefore generate very similar total correlation maps. However, by eliminating shared influences, one can see a clear difference in localization in the partial correlation maps. If the difference in BOLD signal between the motor/premotor and somatosensory cortices were strictly the result of scanner noise or widely distributed physiological noise, elimination of one signal from the other would result in a correlation map with little specificity. Instead, elimination of shared signals demonstrated that the signal unique to each cortical area localized to distinct loci in the thalamus. The observation of increased specificity using a component of the signal unique to each cortical ROI suggests,

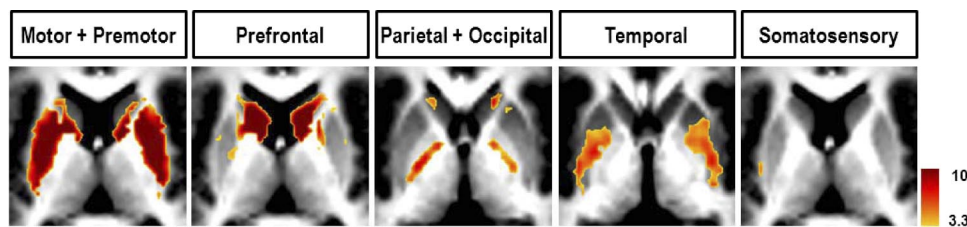


FIG. 3. The basal ganglia system shows high specificity in correlational connectivity with the cortex. Motor and premotor cortex are most correlated with putamen and juxtaposing head of caudate nucleus (slice: $z = 10$). Prefrontal cortex is most correlated with caudate nucleus (slice: $z = 10$). Parietal and occipital cortex have weaker but seemingly specific correlations with parts of globus pallidus, mostly confined to the internal segment (slice: $z = 2$). Temporal cortex has weak correlations with parts of putamen ($z = 0$). Somatosensory ($z = 10$).

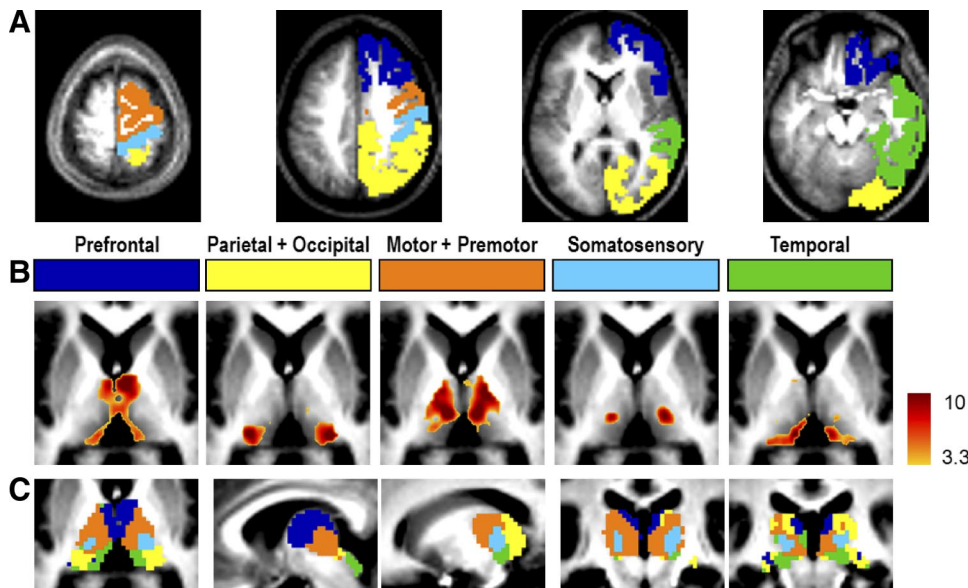


FIG. 4. *A*: unilateral cortical ROIs in the right hemisphere demonstrate the same specificity as bilateral cortical ROIs in ipsilateral as well as contralateral thalamus. All else as in Fig. 1*A*. *B*: corresponding partial correlation Z-score maps. All else as in Fig. 1*B*. *C*: WTA maps. All else as in Fig. 1*C*.

first, that this component is of neuronal origin and, second, that partial correlation offers a way to isolate components of neuronal activity from a mixture of recorded neuronal signals.

DISCUSSION

Spontaneous coherent fluctuations in both brain oxygen availability and blood flow in the cerebral cortex of a variety of species including humans have been known for >30 yr (for a review of this interesting early literature see Vern et al. 1997). Because the fMRI BOLD signal is dependent on changes in oxygen availability (Ogawa et al. 1990; Pauling and Coryell 1936a,b; Thulborn et al. 1982) it follows that the BOLD signal should contain evidence of such spontaneous coherent fluctuations. It was Biswal and colleagues (1995) who first demonstrated that spontaneous fluctuations in the fMRI BOLD signal (i.e., “noise”) contained evidence of spatially coherent fluctuations in brain oxygen availability. Since then, there has been increasing interest in this long overlooked phenomenon. It is now clear that the spatial organization of this intrinsic activity replicates the topography of multiple brain systems of the human and monkey cerebral cortex previously defined on the basis of task-related neuroimaging (for a recent review see Fox and Raichle 2007). However, the majority of this work has focused on the cerebral cortex.

Herein we show that the spatial organization of the brain’s intrinsic neuronal activity, as reflected in spontaneous fluctuations of the fMRI BOLD signal (Leopold et al. 2003; Logothetis et al. 2001), includes highly organized patterns of coherent activity shared by the thalamus and the cerebral cortex. The present results (Fig. 1 and Supplemental Fig. S2) define thalamocortical relationships in substantial agreement with known thalamic nuclear grouping determined by postmortem human studies (Mai et al. 2008; Morel et al. 1997) and anatomical track-tracing data from other mammalian species including monkeys (Jones 2007; Nieuwenhuys et al. 1988). Our results, however, are not expected to correspond exactly to anatomical studies because partial correlation mapping of the BOLD signal is fundamentally a physiological as opposed to an anatomical technique that measures modulation of neuronal activity (Logothetis et al. 2001; Raichle and Mintun 2006).

Functional and anatomical connectivity

A striking disparity between structure and function is seen in the almost exact mirror symmetry of thalamic maps generated using unilateral cortical ROIs (Fig. 4*B* and Supplemental Fig. S4*B*). This symmetry is not in accordance with known monosynaptic anatomical connectivity between the cortex and the thalamus, which is strongly ipsilateral (Jones 2007). Direct interthalamic connections between principal nuclei have not been shown to exist (Jones 2007) and are thus unlikely to contribute to interthalamic synchrony. Thus it appears most likely that this synchrony is mediated by polysynaptic mechanisms. The cerebral hemispheres are densely interconnected by the major cortical commissures, especially the corpus callosum. The brain stem reticular formation is also well situated to promote symmetry of cortico-thalamic functional relations because it includes multiple bilateral pathways and is densely interconnected with both the thalamus and the cerebral hemispheres (Jones 2007). This bilateral synchrony demonstrates that fMRI BOLD imaging in general allows measurements of functional relationships among areas of the brain that are supported by multisynaptic connections (see Koch et al. 2002; Vincent et al. 2007), whereas anatomical inferences of multisynaptic interactions remain incomplete because of incomplete knowledge of anatomical connectivity (including synaptic organization).

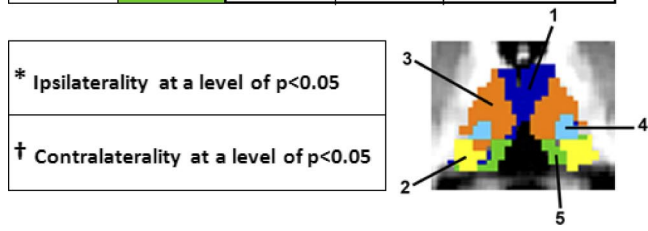
In addition to polysynaptic connections, anatomical and functional/physiological connectivity may produce different results for other reasons. First, structure and function are not expected to have a proportional relationship between the importance of a connection and the number of axonal projections (or synaptic inputs) to a given area, even if future work is able to derive such detailed connectional anatomy for all areas of the brain. For example, retinal input accounts for only 7% of the total synapses to the cat LGN, outnumbered by inputs from cortex and even brain stem, yet few would argue that the LGN functions primarily to relay information from the retina and not brain stem (Sherman and Guillery 2006; Van Horn et al. 2000). Thus driver input to the LGN and other thalamic relay cells in general, which define the information being relayed, may be greatly outnumbered by modulatory input to those same areas

TABLE 1. *Laterality of the strength of thalamic partial correlations with left or right cortical ROIs*

A Left Cortical ROIs				
Thalamic Partition	Color	Laterality Test		
		Left Thal	Right Thal	Paired t-test p
1	Blue	0.1306	0.0720	7x10 ⁻⁷ *
2	Yellow	0.1311	0.1436	0.036 †
3	Orange	0.1115	0.1014	0.048 *
4	Light Blue	0.1034	0.0748	0.039 *
5	Green	0.1229	0.1266	0.65

B Right Cortical ROIs				
Thalamic Partition	Color	Laterality Test		
		Left Thal	Right Thal	Paired t-test p
1	Blue	0.0996	0.1508	5x10 ⁻⁶ *
2	Yellow	0.1175	0.1297	0.092
3	Orange	0.1130	0.1261	0.020 *
4	Light Blue	0.1031	0.1270	0.090
5	Green	0.1263	0.1221	0.67

C Left + Right Cortical ROIs				
Thalamic Partition	Color	Laterality Test		
		Left Thal	Right Thal	Paired t-test p
1	Blue	0.1347	0.1332	0.82
2	Yellow	0.1218	0.1329	0.085
3	Orange	0.1291	0.1293	0.97
4	Light Blue	0.1031	0.1024	0.95
5	Green	0.1192	0.1214	0.82



The average partial correlation strength for each thalamic partition (color code as in Fig. 1B) was evaluated in each hemithalamus. The statistical results represent paired *t*-tests (two-sided) over the population of subjects computed on Fisher's *r*-to-*z* transformed partial correlations, the null hypothesis being equal to the mean partial correlation in the left and right hemithalamus. Asterisks (*) indicate ipsilaterality significance exceeding $P < 0.05$. Daggers (†) indicate contralaterality significance exceeding $P < 0.05$. Note: statistically significant prefrontal ipsilaterality but absent temporal ipsilaterality.

(Sherman and Guillery 2006; Wang et al. 2002). Drivers may be able to exert a dominant role in downstream signaling because of distinct synaptic properties different from modulators (terminal arbor morphology, neurotransmitter type, probability of transmitter release, ionotropic vs. metabotropic receptor activation) (Sherman and Guillery 2006).

The distinction between drivers versus modulators is particularly relevant for sensory relay nuclei of the thalamus. Here it is well established that drivers control receptive field properties of relay cells, whereas modulators have little influence on that property (Sherman and Guillery 2006). In higher-order relay

circuits that traverse a cortico-thalamo-cortical pathway, drivers are harder to define in terms of receptive field properties. However, other functional properties of sensory relay drivers may still apply. The functional dominance of retinal input can be seen in the elicitation of larger excitatory postsynaptic potentials in the LGN than modulatory input from layer 6 cortex (Sherman and Guillery 2006). Extending this observation, one can make the argument that the significance of a functional linkage might be observed as a tighter coupling in neuronal activity, especially in relay nuclei where local processing of the signal may be minimal. Intralaminar nuclei show strong correlations with motor and prefrontal cortex in our partial correlation maps, whereas anatomically these thalamic nuclei have diffuse projections to cortex and have been shown to project predominantly to subcortical instead of cortical structures (Jones 2007). Strong correlated activity may suggest a driver-like role in the neuronal circuitry that functionally ties these regions together, even though the number of physical connections may be sparse.

Differences between structure and function may also exist for technical reasons. Our results, being constrained by the spatial resolution of fMRI, are admittedly coarse compared with the level of detail available from formal anatomical studies. Boundaries defined by our cortical partitioning also greatly simplify the level of detail in the anatomical connectivity. Thalamic nuclei have varying degrees of distributional connectivity to multiple cortical regions (Jones 2007), some of which do not respect the boundaries we have defined here. However, the advantage of the functional imaging approach used here compared with classical anatomical studies is that it provides a measure of functional connectivity for every voxel in the thalamus and does so noninvasively in awake, resting humans.

In future work, a combination of functional and anatomical techniques will be best suited to answering questions of functional relationships and fiber pathways contributing to functional synchrony. It is worth noting that a prominent study (Behrens et al. 2003) has previously characterized connections between the cortex and thalamus using diffusion tensor imaging and tractography (DTI/DTT). Although a detailed compar-

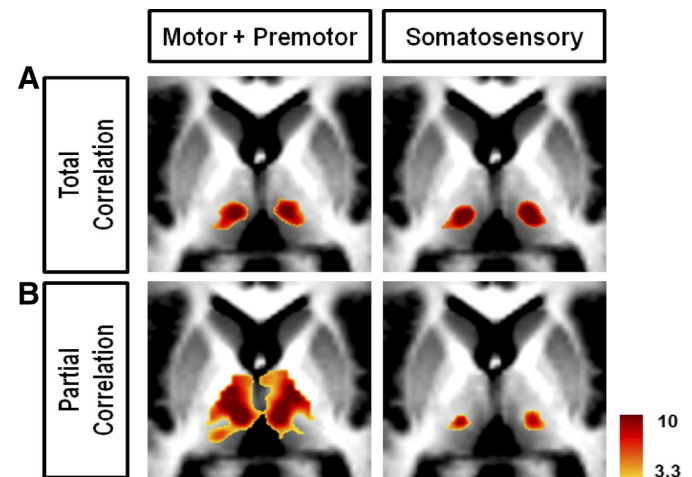


FIG. 5. Comparison of correlation mapping techniques illustrated using the Motor + Premotor and Somatosensory bilateral cortical ROIs shows the increased specificity using partial correlation. A: total correlation. B: partial correlation. All slices are transverse, $z = 6$.

ison of partial correlation mapping versus probabilistic DTT is beyond the scope of this report, we emphasize here that the two methods are based on radically dissimilar approaches that start at opposite ends of the structure/function spectrum and offer two distinct and unique sets of information. DTT uses diffusion-weighted anisotropy to reconstruct fiber tracts on which inferences of functional interactions are possible, whereas partial correlation mapping is able to directly measure functional interactions but not the underlying anatomical pathway that led to the observed synchrony. Therefore an obvious complement exists between the two approaches toward understanding physiologically important functional interactions.

Functional connectivity of the basal ganglia

Functional connections between motor/premotor cortex and putamen and also between prefrontal cortex and caudate are consistent with the anatomical observations from both primates and human studies, demonstrating that the basal ganglia have an important role in motor control and cognition (Middleton and Strick 1994; Mink 1996; Wiesendanger et al. 2004). However, the lack of any correlation between these cortical areas and the globus pallidus (GP) was unexpected given the strong physical connections that the GP receives from the striatum, which in turn receives major projections from the frontal lobe. The lack of any observable functional association may be due to different sensitivity of fMRI measurements to glutamatergic versus GABAergic neurotransmission. The dependence of the fMRI BOLD signal on changes in local oxygen availability sensitizes the method to differences in metabolic needs including differences due to neurotransmitter recycling. Previous studies have shown that astrocyte exposure to glutamate, but not to γ -aminobutyric acid (GABA), elicits glycolysis (Buzsáki et al. 2007; Chatton et al. 2003). It follows from this observation that BOLD fMRI may be much more sensitive to glutamatergic than to GABAergic signaling. Additionally, this signal is more correlated with the neuronal activity input to a given region than the neuronal spiking that is the output of that region (Logothetis et al. 2001; Raichle and Mintun 2006).

Proceeding, for the moment, with the assumption that the fMRI signal reflects glutamatergic more than GABAergic signaling and that the signal seen in a region reflects upstream input, then the activity seen in the globus pallidus likely reflects the neuronal activity of regions of the brain that project excitatory terminals to GP. Because fMRI may not be very sensitive to GABA signaling and because GABAergic synapses compared with glutamatergic synapses likely dominate the total number of synapses in the GP, the predominant activity in the globus pallidus may go undetected in fMRI measurements. Therefore it is possible that the fMRI signal detects activity only from the remaining excitatory pathways, even though these pathways may contribute to only a small portion of the total connectivity to the GP. Anatomically, the GP receives glutamatergic input from subthalamic nucleus, although most of its input is GABAergic from the striatum. In comparing our functional connectivity among structures in the basal ganglia, it seems that, qualitatively, the correlations between GP and occipital/parietal cortex are much weaker than the correlations between the striatum and the cerebral cortex.

Intrinsic activity

Within the thalamocortical circuit, task-evoked activity can produce specific paired activations in the thalamus and cortex such as those in LGN/visual cortex (Kastner et al. 2006) and MGN/auditory cortex (Sigalovsky and Melcher 2006). Although our cortical ROIs encompass large regions of cerebral cortex, the pattern of correlations between these cortical regions and the thalamus shows a similar organization. This spatial overlap of spontaneous activity with evoked activity has been previously reported in cortical systems (Greicius et al. 2003; Hampson et al. 2002; Vincent et al. 2007) and suggests, along with our present data, that functional correlations are preserved in the thalamocortical system during resting state in the absence of overt task performance and even under anesthesia (Vincent et al. 2007). Correlated ongoing spontaneous activity may be required to maintain the integrity of functional relationships and to keep the system in a state of readiness to react to external stimuli and possibly to predict future events (Fox and Raichle 2007).

Thalamocortical system and disease

The importance of the thalamus in maintaining conscious experience is underscored by the recent well-publicized result in which a patient who had been in a minimally conscious state for many years following traumatic brain injury showed dramatic improvement with thalamic stimulation (Schiff et al. 2007). Other data acquired from a persistent vegetative state patient showed alterations in thalamocortical blood flow positron emission tomography measurements that recovered after restoration of consciousness (Laureys et al. 2000). Functional connectivity using resting-state fMRI also shows the promise of detecting alterations in thalamocortical connectivity in patient populations such as those with psychiatric diseases (Anand et al. 2005; Greicius et al. 2007). The thalamic boundaries defined in the present study may serve as a functional atlas for localizing areas of the thalamus that show functional alterations with disease. Systematic characterization of thalamocortical connectivity using similar approaches to the current study may show better localization of thalamic connectivity alterations than have been previously reported.

Future applications of partial correlation mapping

In our analysis, partial correlation offered the advantage of controlling for the specific influences of a priori selected regions of the brain in an attempt to better separate the relative contributions of each cortical signal to thalamic activity. The increase in specificity compared with traditional correlation maps was exemplified in the comparison of motor/premotor and somatosensory maps (Fig. 5). However, many functional connectivity mapping studies are more exploratory and selection of appropriate regions to control for is not possible. Therefore partial correlation mapping is not a technique that would universally replace standard functional connectivity techniques but, rather, a complementary approach in cases where controlling for a priori selected regions is desired.

The partial correlation results presented here (e.g., Fig. 1) were computed after elimination of shared signals from all but one selected cortical ROI. The involved computations may become numerically unstable (and thus generate nonphysi-

ologic results) if any signals to be eliminated are strongly correlated. Thus data suitable for partial correlation analysis must be selected with care to obtain interpretable results. In practice, this places a limit on the number of ROIs that can be used to compute partial correlation maps of the type presented here. Exploratory experiments addressing this question suggest that the ROI count limit may be on the order of 10 (D Zhang and AZ Snyder, unpublished observations). This value will be greater or smaller depending on the quality of the available data (signal-to-noise ratio) and number of subjects available for averaging.

The type and number of signals to be eliminated in computing partial correlations should be defined to fit the needs of the particular analysis of interest. Even after defining these regions, there are combinatoric considerations to take into account. Total correlation is equivalent to partial correlation of order zero (order in this case meaning the number of signals to be eliminated). Partial correlation of order k involves evaluating the determinants of $(k + 1) \times (k + 1)$ submatrices. This mathematical formalism represents a potential framework for organizing the investigation of the brain's internal dialog. Thus given n nodes, there are $1/2(n)(n - 1)$ node pairs, not counting the n instances in which each node is paired with itself. Accordingly, there are $1/2(n)(n - 1)$ total correlations and an equal number of partial correlations of maximal order, the maximal order being $n - 2$. The number of partial correlations of order one is $1/2(n)(n - 1)(n - 2)$. Most generally, the number of partial correlations of order k is $1/2(n)(n - 1)[n - 2k]$, where $\binom{m}{k}$ is the number of ways of selecting k out of m objects.

These combinatoric considerations carry implications regarding the potential uses of partial correlation analysis and apply to any physiological measure of neuronal activity as well as to BOLD imaging. It is evident that the number of defined partial correlations increases faster than exponentially as the number of nodes increases. Even for a handful of nodes, the total number and complexity of potentially computable partial correlations imply that automated methods are needed merely to organize the results. However, we suggest that this complexity is well suited to investigations of the brain in which numerous spontaneous processes maintain communication of varying degrees of specificity versus generality.

GRANTS

This work was supported by National Institutes of Health Grants NS-06833 to M. E. Raichle, F30 MH-083483 to D. Zhang, and K23 HD-053212 to J. S. Shimony.

REFERENCES

- Anand A, Li Y, Wang Y, Wu J, Gao S, Bukhari L, Mathews VP, Kalnin A, Lowe MJ. Activity and connectivity of brain mood regulating circuit in depression: a functional magnetic resonance study. *Biol Psychiatry* 57: 1079–1088, 2005.
- Beckmann CF, DeLuca M, Devlin JT, Smith SM. Investigations into resting-state connectivity using independent component analysis. *Philos Trans R Soc Lond B Biol Sci* 360: 1001–1013, 2005.
- Behrens TE, Johansen-Berg H, Woolrich MW, Smith SM, Wheeler-Kingshott CA, Boulby PA, Barker GJ, Sillery EL, Sheehan K, Ciccarelli O, Thompson AJ, Brady JM, Matthews PM. Non-invasive mapping of connections between human thalamus and cortex using diffusion imaging. *Nat Neurosci* 6: 750–757, 2003.

- Birn RM, Diamond JB, Smith MA, Bandettini PA. Separating respiratory-variation-related fluctuations from neuronal-activity-related fluctuations in fMRI. *Neuroimage* 31: 1536–1548, 2006.
- Biswal B, Yetkin FZ, Haughton VM, Hyde JS. Functional connectivity in the motor cortex of resting human brain using echo-planar MRI. *Magn Reson Med* 34: 537–541, 1995.
- Buzsáki G, Kaila K, Raichle M. Inhibition and brain work. *Neuron* 56: 771–783, 2007.
- Chatton JY, Pellerin L, Magistretti PJ. GABA uptake into astrocytes is not associated with significant metabolic cost: implications for brain imaging of inhibitory transmission. *Proc Natl Acad Sci USA* 100: 12456–12461, 2003.
- Damoiseaux JS, Rombouts SA, Barkhof F, Scheltens P, Stam CJ, Smith SM, Beckmann CF. Consistent resting-state networks across healthy subjects. *Proc Natl Acad Sci USA* 103: 13848–13853, 2006.
- De Luca M, Beckmann CF, De Stefano N, Matthews PM, Smith SM. fMRI resting state networks define distinct modes of long-distance interactions in the human brain. *Neuroimage* 29: 1359–1367, 2006.
- Dosenbach NU, Fair DA, Miezin FM, Cohen AL, Wenger KK, Dosenbach RA, Fox MD, Snyder AZ, Vincent JL, Raichle ME, Schlaggar BL, Petersen SE. Distinct brain networks for adaptive and stable task control in humans. *Proc Natl Acad Sci USA* 104: 11073–11078, 2007.
- Fox MD, Raichle ME. Spontaneous fluctuations in brain activity observed with functional magnetic resonance imaging. *Nat Rev* 8: 700–711, 2007.
- Fox MD, Snyder AZ, Vincent JL, Corbetta M, Van Essen DC, Raichle ME. The human brain is intrinsically organized into dynamic, anticorrelated functional networks. *Proc Natl Acad Sci USA* 102: 9673–9678, 2005.
- Fox MD, Snyder AZ, Vincent JL, Raichle ME. Intrinsic fluctuations within cortical systems account for intertrial variability in human behavior. *Neuron* 56: 171–184, 2007.
- Friston KJ. *Statistical Parametric Mapping: The Analysis of Functional Brain Images*. Amsterdam: Elsevier/Academic Press, 2007.
- Greicius MD, Flores BH, Menon V, Glover GH, Solvason HB, Kenna H, Reiss AL, Schlagberg AF. Resting-state functional connectivity in major depression: abnormally increased contributions from subgenual cingulate cortex and thalamus. *Biol Psychiatry* 62: 429–437, 2007.
- Greicius MD, Krasnow B, Reiss AL, Menon V. Functional connectivity in the resting brain: a network analysis of the default mode hypothesis. *Proc Natl Acad Sci USA* 100: 253–258, 2003.
- Greicius MD, Supekar K, Menon V, Dougherty RF. Resting-state functional connectivity reflects structural connectivity in the default mode network. *Cereb Cortex* (April 9, 2008). doi:10.1093/cercor/bhn059.
- Hampson M, Peterson BS, Skudlarski P, Gatenby JC, Gore JC. Detection of functional connectivity using temporal correlations in MR images. *Hum Brain Mapp* 15: 247–262, 2002.
- Herbert H, Aschoff A, Ostwald J. Topography of projections from the auditory cortex to the inferior colliculus in the rat. *J Comp Neurol* 304: 103–122, 1991.
- Honey CJ, Kotter R, Breakspear M, Sporns O. Network structure of cerebral cortex shapes functional connectivity on multiple time scales. *Proc Natl Acad Sci USA* 104: 10240–10245, 2007.
- Jenkins GM, Watts DG. *Spectral Analysis and Its Applications*. Oakland, CA: Holden-Day, 1968.
- Johnston JM, Vaishnavi SN, Smyth MD, Zhang D, He BJ, Zempel JM, Shimony JS, Snyder AZ, Raichle ME. Loss of resting interhemispheric functional connectivity after complete section of the corpus callosum. *J Neurosci* 28: 6453–6458, 2008.
- Jones EG. *The Thalamus*. Cambridge, UK: Cambridge Univ. Press, 2007, p. 1679.
- Kastner S, Schneider KA, Wunderlich K. Beyond a relay nucleus: neuroimaging views on the human LGN. *Prog Brain Res* 155: 125–143, 2006.
- Koch MA, Norris DG, Hund-Georgiadis M. An investigation of functional and anatomical connectivity using magnetic resonance imaging. *Neuroimage* 16: 241–250, 2002.
- Lancaster JL, Glass TG, Lankipalli BR, Downs H, Mayberg H, Fox PT. A modality-independent approach to spatial normalization of tomographic images of the human brain. *Hum Brain Mapp* 3: 209–223, 1995.
- Laureys S, Faymonville ME, Luxen A, Lamy M, Franck G, Maquet P. Restoration of thalamocortical connectivity after recovery from persistent vegetative state. *Lancet* 355: 1790–1791, 2000.
- Leopold DA, Murayama Y, Logothetis NK. Very slow activity fluctuations in monkey visual cortex: implications for functional brain imaging. *Cereb Cortex* 13: 422–433, 2003.
- Lock TM, Baizer JS, Bender DB. Distribution of corticotectal cells in macaque. *Exp Brain Res* 151: 455–470, 2003.

- Logothetis NK, Pauls J, Augath M, Trinath T, Oeltermann A.** Neurophysiological investigation of the basis of the fMRI signal. *Nature* 412: 150–157, 2001.
- Mai J, Paxinos G, Voss T.** *Atlas of the Human Brain*. Amsterdam: Elsevier/Academic Press, 2008.
- Middleton FA, Strick PL.** Anatomical evidence for cerebellar and basal ganglia involvement in higher cognitive function. *Science* 266: 458–461, 1994.
- Mink JW.** The basal ganglia: focused selection and inhibition of competing motor programs. *Prog Neurobiol* 50: 381–425, 1996.
- Morel A, Magnin M, Jeanmonod D.** Multiarchitectonic and stereotactic atlas of the human thalamus. *J Comp Neurol* 387: 588–630, 1997.
- Nieuwenhuys R, Voogd J, van Huijzen C.** *The Human Central Nervous System: A Synopsis and Atlas*. New York: Springer-Verlag, 1988.
- Ogawa S, Lee TM, Kay AR, Tank DW.** Brain magnetic resonance imaging with contrast dependent on blood oxygenation. *Proc Natl Acad Sci USA* 87: 9868–9872, 1990.
- Ojemann JG, Akbudak E, Snyder AZ, McKinstry RC, Raichle ME, Conturo TE.** Anatomic localization and quantitative analysis of gradient refocused echo-planar fMRI susceptibility artifacts. *Neuroimage* 6: 156–167, 1997.
- Pauling L, Coryell CD.** The magnetic properties and structure of hemoglobin, oxyhemoglobin and carbonmonoxyhemoglobin. *Proc Natl Acad Sci USA* 22: 210–216, 1936a.
- Pauling L, Coryell CD.** The magnetic properties and structure of the hemochromogens and related substances. *Proc Natl Acad Sci USA* 22: 159–163, 1936b.
- Quigley M, Cordes D, Turski P, Moritz C, Haughton V, Seth R, Meyerand ME.** Role of the corpus callosum in functional connectivity. *Am J Neuro-radiol* 24: 208–212, 2003.
- Raichle ME, Mintun MA.** Brain work and brain imaging. *Annu Rev Neurosci* 29: 449–476, 2006.
- Roger M, Arnault P.** Anatomical study of the connections of the primary auditory area in the rat. *J Comp Neurol* 287: 339–356, 1989.
- Rowland DJ, Garbow JR, Laforest R, Snyder AZ.** Registration of [18F]FDG microPET and small-animal MRI. *Nucl Med Biol* 32: 567–572, 2005.
- Schiff ND, Giacino JT, Kalmar K, Victor JD, Baker K, Gerber M, Fritz B, Eisenberg B, O'Connor J, Kobylarz EJ, Farris S, Machado A, McCagg C, Plum F, Fins JJ, Rezai AR.** Behavioural improvements with thalamic stimulation after severe traumatic brain injury. *Nature* 448: 600–603, 2007.
- Seeley WW, Menon V, Schatzberg AF, Keller J, Glover GH, Kenna H, Reiss AL, Greicius MD.** Dissociable intrinsic connectivity networks for salience processing and executive control. *J Neurosci* 27: 2349–2356, 2007.
- Sherman SM, Guillery RW.** *Exploring the Thalamus and Its Role in Cortical Function*. Cambridge, MA: MIT Press, 2006.
- Sigalovsky IS, Melcher JR.** Effects of sound level on fMRI activation in human brainstem, thalamic and cortical centers. *Hear Res* 215: 67–76, 2006.
- Stein T, Moritz C, Quigley M, Cordes D, Haughton V, Meyerand E.** Functional connectivity in the thalamus and hippocampus studied with functional MR imaging. *Am J Neuroradiol* 21: 1397–1401, 2000.
- Talairach J, Tournoux P.** *Co-Planar Stereotaxic Atlas of the Human Brain. 3-Dimensional Proportional System: An Approach to Cerebral Imaging*. New York: Thieme, 1988.
- Thulborn KR, Waterton JC, Matthews PM, Radda GK.** Oxygenation dependence of the transverse relaxation time of water protons in whole blood at high field. *Biochim Biophys Acta* 714: 265–270, 1982.
- Triantafyllou C, Hoge RD, Krueger G, Wiggins CJ, Potthast A, Wiggins GC, Wald LL.** Comparison of physiological noise at 1.5 T, 3 T and 7 T and optimization of fMRI acquisition parameters. *Neuroimage* 26: 243–250, 2005.
- Van Essen DC.** A population-average, landmark- and surface-based (PALS) atlas of human cerebral cortex. *Neuroimage* 28: 635–662, 2005.
- Van Essen DC, Drury HA.** Structural and functional analyses of human cerebral cortex using a surface-based atlas. *J Neurosci* 17: 7079–7102, 1997.
- Van Essen DC, Drury HA, Dickson J, Harwell J, Hanlon D, Anderson CH.** An integrated software suite for surface-based analyses of cerebral cortex. *J Am Med Inform Assoc* 8: 443–459, 2001.
- Van Horn SC, Erisir A, Sherman SM.** Relative distribution of synapses in the A-laminae of the lateral geniculate nucleus of the cat. *J Comp Neurol* 416: 509–520, 2000.
- Vern BA, Leheta BJ, Juel VC, LaGuardia J, Graupe P, Schuette WH.** Interhemispheric synchrony of slow oscillations of cortical blood volume and cytochrome aa3 redox state in unanesthetized rabbits. *Brain Res* 775: 233–239, 1997.
- Vincent JL, Patel GH, Fox MD, Snyder AZ, Baker JT, Van Essen DC, Zempel JM, Snyder LH, Corbetta M, Raichle ME.** Intrinsic functional architecture in the anaesthetized monkey brain. *Nature* 447: 83–86, 2007.
- Wang S, Eisenback MA, Bickford ME.** Relative distribution of synapses in the pulvinar nucleus of the cat: implications regarding the “driver/modulator” theory of thalamic function. *J Comp Neurol* 454: 482–494, 2002.
- Weatherburn CE.** *A First Course in Mathematical Statistics* (2nd ed.). Cambridge, UK: Cambridge Univ. Press, 1949.
- Wiesendanger E, Clarke S, Kraftsik R, Tardif E.** Topography of cortico-striatal connections in man: anatomical evidence for parallel organization. *Eur J Neurosci* 20: 1915–1922, 2004.
- Woods RP, Grafton ST, Holmes CJ, Cherry SR, Mazziotta JC.** Automated image registration: I. General methods and intrasubject, intramodality validation. *J Comput Assist Tomogr* 22: 139–152, 1998.